

## Fluoro Derivatives of Retinal Illuminate the Decisive Role of the C<sub>12</sub>-H Element in Photoisomerization and Rhodopsin Activation

Petra H. M. Bovee-Geurts,<sup>†</sup> Isabelle Fernández Fernández,<sup>‡</sup> Robert S. H. Liu,<sup>§</sup>  
Richard A. Mathies,<sup>||</sup> Johan Lugtenburg,<sup>‡</sup> and Willem J. DeGrip<sup>\*,†,‡</sup>

*Department of Biochemistry, UMCN 286, Nijmegen Centre for Molecular Life Sciences, Radboud University Nijmegen Medical Centre, P.O. Box 9101, 6500 HB Nijmegen, The Netherlands, Department of BioOrganic Photochemistry, Leiden Institute of Chemistry, Leiden University, P.O. Box 9502, 2300 RA Leiden, The Netherlands, Department of Chemistry, University of Hawaii at Manoa, 2545 The Mall, Honolulu, Hawaii 96822, and Department of Chemistry, University of California, Berkeley, California 94720*

Received September 7, 2009; E-mail: wdgrjp@ru.nl

**Abstract:** Rhodopsin, the visual pigment of the vertebrate rod cell, is among the best investigated members of the G-protein-coupled receptor family. Within this family a unique characteristic of visual pigments is their covalently bound chromophore, 11-*cis* retinal, which acts as an inverse agonist. Upon illumination it can be transformed into the all-*trans* isomer that acts as a full agonist. This photoisomerization process is extremely efficient: 2 out of 3 photons are effective, full stereoselectivity is achieved, and stereoinversion occurs within 200 fs. The mechanism behind this process is still not really understood, although the available evidence points at the twisted C<sub>9</sub>–C<sub>13</sub> segment of the 11-*cis* ligand as the quintessence. To further dissect the role of this segment, we have generated the 10-fluoro, 12-fluoro, and 14-fluoro analogues of rhodopsin. A fluoro substituent brings in only little more volume than hydrogen, but considerably more mass and polarizability. The analogue pigments were compared to rhodopsin with respect to their photosensitivity (quantum yield), light-induced structural transitions (UV–vis and FT-IR spectroscopy), and signaling activity (G protein activation rate). We find that 14-F substitution is quite neutral, while 10-F and 12-F substitutions exert significant but distinct effects. The 10-F pigment exhibits a quantum yield similar to that of rhodopsin (0.65) but strongly perturbed thermodynamics of the structural transitions following photoactivation and only 20% of the native signaling activity. The 12-F pigment exhibits a significantly decreased quantum yield (0.47) and signaling activity (30%) but mixed effects on the structural transitions. These properties are compared to those of the corresponding methyl derivatives. We conclude that rotation of the C<sub>12</sub>-H bond of the rhodopsin chromophore is a major rate-limiting factor in the photoisomerization process, while the C<sub>10</sub>-H moiety plays a dominant role in ligand relaxation and further rearrangements following photoactivation.

### Introduction

Rhodopsin is the visual pigment of the rod photoreceptor cells in the vertebrate retina, which mediate dim-light vision.<sup>1–3</sup> As a member of the superfamily of G-protein-coupled receptors, rhodopsin is specialized for reception of photons in such a way that its ligand is the photosensory element (chromophore) and has become covalently bound to the apoprotein, opsin. This ligand is 11-*cis* retinal (Figure 1), a derivative of vitamin A, which is attached in the opsin binding site to Lys-296 through

formation of a protonated Schiff base<sup>1,4–6</sup> that is stabilized by a nearby located counterion in the form of a glutamate residue of opsin (Glu-113). The 11-*cis* isomer acts as a potent inverse agonist of opsin, practically eliminating its basal activity, but is converted by light into the all-*trans* configuration that acts as a full agonist.<sup>2,7</sup> This light-triggered isomerization of the ligand induces conformational changes in the protein, which are driven by about 35 kcal of photon energy stored in the photoproduct Batho.<sup>8–10</sup> This culminates within several milliseconds via a cascade of intermediates in generation of the

<sup>†</sup> Radboud University Nijmegen Medical Centre.

<sup>§</sup> University of Hawaii at Manoa.

<sup>||</sup> University of California, Berkeley.

<sup>‡</sup> Leiden Institute of Chemistry.

(1) Wald, G. *Nature* **1968**, *219*, 800–807.

(2) Ernst, O. P.; Hofmann, K. P.; Palczewski, K. In *Photoreceptors and Light Signalling*; Batschauer, A., Ed.; Royal Society of Chemistry: Cambridge, U.K., 2003; pp 77–123.

(3) Palczewski, K. *Annu. Rev. Biochem.* **2006**, *75*, 743–767.

(4) Bownds, M. D. *Nature* **1967**, *216* (121), 1178–1181.

(5) Eyring, G.; Mathies, R. A. *Proc. Natl. Acad. Sci. U.S.A.* **1979**, *76* (1), 33–37.

(6) Wang, K.; McDowell, J. H.; Hargrave, P. A. *Biochemistry* **1980**, *19* (22), 5111–5117.

(7) Hofmann, K. P. In *Molecular Mechanisms in Visual Transduction*; Stavenga, D. G., DeGrip, W. J., Pugh, E. N., Jr., Eds.; Elsevier Science: Amsterdam, The Netherlands, 2000; pp 91–142.

(8) Cooper, A. *Nature* **1979**, *282*, 531–533.

(9) Schick, G. A.; Cooper, T. M.; Holloway, R. A.; Murray, L. P.; Birge, R. R. *Biochemistry* **1987**, *26* (9), 2556–2562.

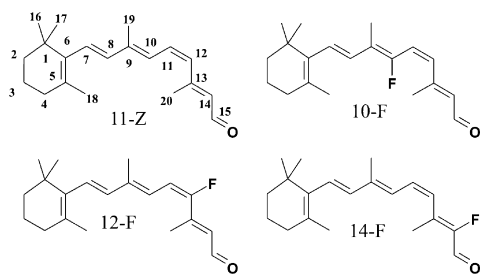


**Figure 1.** Chemical structure of 11-*cis* retinal (11-Z) and the fluoro derivatives used in this study. The structures are shown in the 12-*s trans* conformation, which is dictated by the opsin binding pocket.

active state, Meta II, that binds and activates its cognate G protein transducin.<sup>7,11</sup> Next to their rate of formation, the intermediates in this cascade (Batho  $\leftrightarrow$  blue-shifted intermediate (BSI)  $\rightarrow$  Lumi  $\rightarrow$  Meta I  $\leftrightarrow$  Meta II) can be distinguished by their spectral properties and can be isolated by cryotrapping.<sup>1,12–14</sup>

The photochemical performance of the 11-*cis* retinal–opsin couple is quite remarkable. Photoisomerization occurs with an unprecedented quantum yield ( $0.65 \pm 0.02$ ) in a truly selective reaction pathway (11-*cis*  $\rightarrow$  all-*trans*), generating within 200 fs a vibrationally hot intermediate (photorhodopsin) with a highly distorted but already all-*transoid* chromophore, which within 1 ps proceeds to Batho containing a still highly strained all-*trans* chromophore.<sup>15–19</sup>

According to a variety of resonance Raman, solid-state NMR, and computational studies, the C<sub>10</sub>H and C<sub>12</sub>H elements play special roles in the photoisomerization of the rhodopsin chromophore.<sup>16,20–30</sup> The crystal structure of the first photoproduct Batho also suggests that the C<sub>10</sub>-H and C<sub>12</sub>-H bonds have proceeded through major

twists during photoisomerization.<sup>17,31</sup> Methyl substituents at these positions moderately to severely affect the quantum yield of the photoreaction, the thermodynamics of the subsequent thermal reactions and the signaling activity of the photoactivated pigment.<sup>32,33</sup> On the other hand, the 11–19 ethano-derivative of retinal, which severely restricts the rotational freedom of the C<sub>10</sub>H moiety, only moderately affects the kinetics of the photocascade.<sup>34,35</sup> Hence, this questions whether photoactivation triggers major structural rearrangements in the C<sub>9</sub>–C<sub>11</sub> moiety of the chromophore.

To further elucidate the special contribution of the C<sub>10</sub>H and C<sub>12</sub>H sites to photoactivation of rhodopsin, we introduced a fluorine label at either position. This label is not much larger than the hydrogen at this position but much smaller than a methyl group (van der Waals radii of about 0.14, 0.12, and 0.20 nm, respectively<sup>36,37</sup>), while its molecular mass is even larger than that of a methyl group (19.0 versus 15.0 Da). In addition fluorine is a very sensitive NMR label.

Since methyl and fluoro derivatives at the C<sub>14</sub> position hardly affect the signaling properties of rhodopsin,<sup>38–40</sup> we exploited the 14-F analogue as a reference. The structures of native 11-*cis* retinal and the three 11-*cis* fluororetinals used in this study are presented in Figure 1. The 10-F, 12-F, and 14-F fluoroanalogues of rhodopsin have been successfully prepared before,<sup>41,42</sup> but their analysis has so far been restricted to their spectral properties and to preliminary photochemical and solution-state NMR studies.<sup>38,40–44</sup>

Our objectives are to characterize for the three fluororhodopsins the photoreaction (Rho  $\rightarrow$  Batho) and subsequent thermal reaction cascade generating Meta II in comparison to native rhodopsin in order to further enlighten the contribution of the C<sub>10</sub>H and C<sub>12</sub>H elements of the chromophore to photoisomerization and activation of rhodopsin. We have determined the

- (10) Birge, R. R.; Vought, B. W. *Methods Enzymol.* **2000**, *315*, 143–163.
- (11) Kühn, H. *Prog. Retinal Eye Res.* **1984**, *3*, 123–156.
- (12) Yoshizawa, T.; Wald, G. *Nature* **1963**, *197*, 1279–1286.
- (13) Yoshizawa, T. *Adv. Biophys.* **1984**, *17*, 5–67.
- (14) Kliger, D. S.; Lewis, J. W. *Isr. J. Chem.* **1995**, *35* (3–4), 289–307.
- (15) Mathies, R. A.; Lugtenburg, J. In *Molecular Mechanisms in Visual Transduction*; Stavenga, D. G., DeGrip, W. J., Pugh, E. N., Jr., Eds.; Elsevier Science: Amsterdam, The Netherlands, 2000; pp 55–90.
- (16) Kukura, P.; McCamant, D. W.; Yoon, S.; Wandschneider, D. B.; Mathies, R. A. *Science* **2005**, *310* (5750), 1006–1009.
- (17) Nakamichi, H.; Okada, T. *Angew. Chem., Int. Ed.* **2006**, *45* (26), 4270–4273.
- (18) Wang, Q.; Schoenlein, R. W.; Peteanu, L. A.; Mathies, R. A.; Shank, C. V. *Science* **1994**, *266* (5184), 422–424.
- (19) Kandori, H.; Furutani, Y.; Nishimura, S.; Shichida, Y.; Chosrowjan, H.; Shibata, Y.; Mataga, N. *Chem. Phys. Lett.* **2001**, *334* (4–6), 271–276.
- (20) Bifone, A.; de Groot, H. J. M.; Buda, F. *J. Phys. Chem. B* **1997**, *101* (15), 2954–2958.
- (21) Creemers, A. F. L.; Kiihne, S. R.; Bovee-Geurts, P. H. M.; DeGrip, W. J.; Lugtenburg, J.; de Groot, H. J. M. *Proc. Natl. Acad. Sci. U.S.A.* **2002**, *99* (14), 9101–9106.
- (22) Yan, E. C. Y.; Ganim, Z.; Kazmi, M. A.; Chang, B. S. W.; Sakmar, T. P.; Mathies, R. A. *Biochemistry* **2004**, *43* (34), 10867–10876.
- (23) Gascón, J. A.; Sproviero, E. M.; Batista, V. S. *Acc. Chem. Res.* **2006**, *39* (3), 184–193.
- (24) Crozier, P. S.; Stevens, M. J.; Woolf, T. B. *Proteins: Struct., Funct., Bioinf.* **2007**, *66* (3), 559–574.
- (25) Frutos, L. M.; Andruniów, T.; Santoro, F.; Ferré, N.; Olivucci, M. *Proc. Natl. Acad. Sci. U.S.A.* **2007**, *104* (19), 7764–7769.
- (26) Weingart, O. *J. Am. Chem. Soc.* **2007**, *129* (35), 10618–10619.
- (27) Coto, P. B.; Strambi, A.; Olivucci, M. *Chem. Phys.* **2008**, *347* (1–3), 483–491.
- (28) Tomasello, G.; Olaso-González, G.; Altoè, P.; Stenta, M.; Serrano-Andrés, L.; Merchán, M.; Orlandi, G.; Bottoni, A.; Garavelli, M. *J. Am. Chem. Soc.* **2009**, *131* (14), 5172–5186.
- (29) Hayashi, S.; Taikhorshid, E.; Schulten, K. *Biophys. J.* **2009**, *96* (2), 403–416.

- (30) Gansmüller, A.; Concistrè, M.; McLean, N.; Johannessen, O. G.; Marín-Montesinos, I.; Bovee-Geurts, P. H. M.; Verdegem, P. J. E.; Lugtenburg, J.; Brown, R. C. D.; DeGrip, W. J.; Levitt, M. H. *Biochim. Biophys. Acta, Biomembr.* **2009**, *1788* (6), 1350–1357.
- (31) Schreiber, M.; Sugihara, M.; Okada, T.; Buss, V. *Angew. Chem., Int. Ed.* **2006**, *45* (26), 4274–4277.
- (32) DeLange, F.; Bovee-Geurts, P. H. M.; VanOostrum, J.; Portier, M. D.; Verdegem, P. J. E.; Lugtenburg, J.; DeGrip, W. J. *Biochemistry* **1998**, *37*, 1411–1420.
- (33) Verhoeven, M. A.; Bovee-Geurts, P. H. M.; de Groot, H. J. M.; Lugtenburg, J.; DeGrip, W. J. *J. Mol. Biol.* **2006**, *363* (1), 98–113.
- (34) Sheves, M.; Albeck, A.; Ottolenghi, M.; Bovee-Geurts, P. H. M.; DeGrip, W. J.; Einterz, C. M.; Lewis, J. W.; Schaechter, L. E.; Kliger, D. S. *J. Am. Chem. Soc.* **1986**, *108*, 6440–6441.
- (35) Lewis, J. W.; Pinkas, I.; Sheves, M.; Ottolenghi, M.; Kliger, D. S. *J. Am. Chem. Soc.* **1995**, *117* (3), 918–923.
- (36) Pauling, L. *The Nature of the Chemical Bond and the Structure of Molecules and Crystals: An Introduction to Modern Structural Chemistry*, 3rd (rev) ed.; Cornell University Press: Ithaca, NY, 1960.
- (37) Bondi, A. *J. Phys. Chem.* **1964**, *68* (3), 441–451.
- (38) Liu, R. S. H.; Denny, M.; Zingoni, J. P.; Mead, D.; Matsumoto, H.; Asato, A. E. In *Biophysical Studies of Retinal Proteins*; Ebrey, T. G., Frauenfelder, H., Honig, B., Nakanishi, K., Eds.; University of Illinois Press: Champaign, IL, 1987; pp 59–63.
- (39) Karnaukhova, E. N.; Hu, S. H.; Boonyasai, R.; Tan, Q.; Nakanishi, K. *Bioorg. Chem.* **1999**, *27*, 372–382.
- (40) Vogel, R.; Siebert, F.; Yan, E. C. Y.; Sakmar, T. P.; Hirshfeld, A.; Sheves, M. *J. Am. Chem. Soc.* **2006**, *128* (32), 10503–10512.
- (41) Asato, A. E.; Matsumoto, H.; Denny, M.; Liu, R. S. H. *J. Am. Chem. Soc.* **1978**, *100* (18), 5957–5960.
- (42) Liu, R. S. H.; Matsumoto, H.; Asato, A. E.; Denny, M.; Shichida, Y.; Yoshizawa, T.; Dahlquist, F. W. *J. Am. Chem. Soc.* **1981**, *103*, 7195–7201.
- (43) Shichida, Y.; Ono, T.; Yoshizawa, T.; Matsumoto, H.; Asato, A. E.; Zingoni, J. P.; Liu, R. S. H. *Biochemistry* **1987**, *26* (14), 4422–4428.
- (44) Steinberg, G.; Ottolenghi, M.; Sheves, M. *Biophys. J.* **1993**, *64*, 1499–1502.

quantum yield ( $\Phi$ ) as a measure for the efficiency and rate of the photoisomerization reaction.<sup>16,45,46</sup> The entire photocascade was monitored by means of FT-IR spectroscopy at selected temperatures, since this is the most straightforward way to discriminate between the various intermediate states of the cascade.<sup>47–50</sup> The signaling activity was assayed as the G protein activation rate per photoactivated pigment relative to that of native rhodopsin.

## Experimental Section

**Materials.** All chemicals were of analytical grade. Detergents were obtained from Anatrace (Maumee, OH). Native 11-*cis* retinal was provided by Dr. Rosalie Crouch (Medical University of South Carolina, Charleston, SC) through financial support from NEI.

**Synthesis of Retinals.** The 10-F and 14-F derivatives of all-*trans* retinal were synthesised as described before.<sup>41</sup> The corresponding 11-*cis* isomers were prepared by irradiation of the all-*trans* isomer in acetonitrile and purified by preparative high performance liquid chromatography.<sup>51</sup> The 12-F derivative was prepared in the 11-*cis* configuration also as described before.<sup>42</sup> In this case the C15 precursor was synthesized as a mixture of the all-*trans* and 11-*cis* isomers. The 11-*cis* isomer was isolated by chromatography and extended into the corresponding retinal. The spectral and <sup>1</sup>H NMR characteristics of the three 11-*cis* fluororetinals fully complied with published data.<sup>38,41,42</sup>

**Isolation of Bovine Opsin and Regeneration with 11-*cis* Retinals.** Bovine rod outer segment membranes in the opsin form (opsin membranes) were prepared from fresh, light-adapted cattle eyes as described.<sup>32,52</sup> The regeneration capacity of these preparations was estimated from the  $A_{280}/A_{500}$  ratio measured after subsequent incubation with a 3-fold excess of 11-*cis* retinal, whereby a ratio of  $2.1 \pm 0.1$  was taken to represent membranes with a maximal rhodopsin content. Rhodopsin and the fluororhodopsin analogues were prepared with opsin membranes showing a regeneration capacity in the range 90–100%. Regeneration and further manipulations with the pigments were done under dim red light (>620 nm, Schott RG620 cutoff filter).

Analogue pigments were generated by incubating a suspension of opsin membranes (50–100  $\mu$ M opsin in buffer A: 20 mM PIPES, 130 mM NaCl, 5 mM KCl, 2 mM CaCl<sub>2</sub>, 0.1 mM EDTA, 1 mM DTE, pH 6.5) with a 2- to 3-fold molar excess of the 11-*cis* fluororetinal at room temperature. After 2 h a small aliquot was assayed for the extent of regeneration by addition of 11-*cis* retinal in a 1:1 molar ratio to the original opsin. With all three fluororetinals regeneration was nearly complete; to achieve full regeneration an additional aliquot of the fluororetinal was added, and the incubation was continued overnight at 4 °C. Excess retinal was then converted into the corresponding oxime by addition of a 1 M hydroxylamine solution (pH 6.5) to a final concentration of 10 mM. After cooling in ice and 30 min of incubation, the oxime was largely removed by two extractions with 50 mM heptakis(2,6-di-*O*-methyl)- $\beta$ -cyclodextrin,<sup>32</sup> which, however, also removes some lipids thereby

perturbing the Meta I to Meta II transition. To restore a native lipid/protein ratio, the membrane pellet was dissolved in 20 mM nonylglucoside in buffer A (to ca. 50  $\mu$ M of pigment) by incubation for 1 h on ice. Undissolved material was removed by centrifugation (30 min, 80,000g, 4 °C), and the supernatant was mixed with a solution of asolectin (100 mg/mL in 50 mM nonylglucoside in buffer A) to achieve a 50-fold molar excess of asolectin with respect to pigment. After 15 min of incubation on ice, detergent was extracted by addition of solid  $\beta$ -cyclodextrin to a slight excess over nonylglucose, and the resulting proteoliposomes were isolated by overnight sucrose step-gradient centrifugation at 200,000g and 4 °C as described before.<sup>53</sup> The proteoliposome band was recovered from the 20%/45% sucrose interface, diluted with 2 vol of doubly distilled water, pelleted by centrifugation (60 min, 200,000g, 4 °C), and stored in aliquots under argon in a light-tight container at –80 °C.

**UV–vis Spectroscopy.** The spectral properties of the pigments were determined in micellar solution, by solubilization to about 2.5  $\mu$ M in 20 mM dodecylmaltoide in buffer A containing 10 mM hydroxylamine. The wavelength of maximal absorbance in the visible region ( $\lambda_{\text{max}}$ ) was determined as the peak position in the difference spectrum obtained after subtraction of the spectrum after illumination (300 s; 150 W halogen light through Schott OG530 cutoff filter and fiber optics) from the dark-state spectrum.

The Meta I  $\leftrightarrow$  Meta II equilibrium was analyzed in proteoliposomes using the end-on photomultiplier setup of a Perkin-Elmer Lambda 18 spectrophotometer. Pigments were suspended to about 1  $\mu$ M in buffer of various pH as indicated in the text using MES, MOPS, or Bis-Tris Propane as buffering compound. Samples were maintained at 10 °C by means of a circulating water bath. Spectra were taken before and after illumination (10 s; conditions as above) and then every 5 min up to 30 min after illumination to check for the stability of the Meta photoproducts. Finally, 1 M hydroxylamine was added to a final concentration of 50 mM to convert all photointermediates into the all-*trans* retinaloxime derivative. The relative amount of Meta I at 480 nm remaining immediately after illumination was calculated as described before.<sup>54</sup>

**FT-IR Spectroscopy.** FT-IR analyses were performed on a Bruker IFS 66/S spectrometer, equipped with a liquid nitrogen-cooled, narrow-band HgCdTe (MCT) detector as described.<sup>32,33</sup> In brief, sample temperature was under computer control using a variable-temperature helium-cooled cryostat (Heliostat, APD Cryogenics, Inc.), covered with a set of NaCl windows in the IR light path. Membrane films were prepared by isopotential spin drying<sup>55</sup> 2–3 nmol of pigment in proteoliposomes on AgCl windows (Crystran Limited, U.K.). The membrane film was rehydrated, sealed using a rubber O-ring spacer and a second AgCl window, and screwed tight in the sample holder of the cryostat. Samples were illuminated in the spectrometer using a modified fiber optics ring illuminator (Schott) fed by a 150 W halogen light filtered through a 488( $\pm$ 10) nm interference filter and a long-pass filter (Schott). Routinely, six consecutive blocks of 1280 scans each were recorded at 4 cm<sup>–1</sup> resolution, taking about 120 s acquisition time per block to generate a spectrum, both before and after 2 min of illumination. No differences in pattern for the subsequent spectra were detected and routinely the last dark-state spectrum was subtracted from the first spectrum of the photoproduct to generate a difference spectrum. Habitually, difference spectra were measured at 80, 180, 253, and 283 K, where Batho, Lumi, Meta I, and Meta II, respectively, are sufficiently stable to allow analysis, but if required the temperature range was expanded. Temperature stability was  $\pm 0.2$  K.

(45) Kochendoerfer, G. G.; Verdegem, P. J. E.; Van der Hoef, I.; Lugtenburg, J.; Mathies, R. A. *Biochemistry* **1996**, *35* (50), 16230–16240.

(46) Cembran, A.; Bernardi, F.; Olivucci, M.; Garavelli, M. *Proc. Natl. Acad. Sci. U.S.A.* **2005**, *102* (18), 6255–6260.

(47) Rothschild, K. J.; Cantore, W. A.; Marrero, H. *Science* **1983**, *219*, 1333–1335.

(48) Siebert, F. *Isr. J. Chem.* **1995**, *35* (3–4), 309–323.

(49) DeGrip, W. J.; Rothschild, K. J. In *Molecular Mechanisms in Visual Transduction*; Stavenga, D. G., DeGrip, W. J., Pugh, E. N., Jr., Eds.; Elsevier Science: Amsterdam, The Netherlands, 2000; pp 1–54.

(50) Mahalingam, M.; Martínez-Mayorga, K.; Brown, M. F.; Vogel, R. *Proc. Natl. Acad. Sci. U.S.A.* **2008**, *105* (46), 17795–17800.

(51) Lugtenburg, J. *Pure Appl. Chem.* **1985**, *57* (5), 753–762.

(52) DeGrip, W. J.; VanOostrum, J.; Bovee-Geurts, P. H. M.; VanDerSteen, R.; VanAmsterdam, L.J. P.; Groesbeek, M.; Lugtenburg, J. *Eur. J. Biochem.* **1990**, *191*, 211–220.

(53) DeGrip, W. J.; VanOostrum, J.; Bovee-Geurts, P. H. M. *Biochem. J.* **1998**, *330* (2), 667–674.

(54) DeLange, F.; Merckx, M.; Bovee-Geurts, P. H. M.; Pistorius, A. M. A.; DeGrip, W. J. *Eur. J. Biochem.* **1997**, *243* (1–2), 174–180.

(55) Clark, N. A.; Rothschild, K. J.; Simon, B. A.; Luippold, D. A. *Biophys. J.* **1980**, *31*, 65–96.



**Table 1.** Spectral and Photochemical Properties and Relative G Protein Activation Rates of Rhodopsin and Its Fluoro Derivatives Discussed in This Paper

	native rhodopsin	10-F	12-F	14-F
$\lambda_{\max}$ (nm)	498 $\pm$ 2	502 $\pm$ 2	510 $\pm$ 3	529 $\pm$ 3
$\epsilon_{\max}$ (L/M $\cdot$ cm)	40,600 $\pm$ 1,000	40,000 $\pm$ 3,000	34,000 $\pm$ 4,000	40,000 $\pm$ 3,000
quantum yield	0.65 $\pm$ 0.02 <sup>a</sup>	0.63 $\pm$ 0.12 <sup>b</sup>	0.47 $\pm$ 0.06	0.55 $\pm$ 0.10 <sup>b</sup>
G protein activation (%)	$\equiv$ 100	20 $\pm$ 10	32 $\pm$ 5	$\geq$ 80 <sup>c</sup>

<sup>a</sup> Native quantum yields have been reported (refs 56, 58, 59). <sup>b</sup> Quantum yields of 10-F and 14-F rhodopsin have been reported before (ref 38). <sup>c</sup> Signaling activity of 14-substituted rhodopsins has been reported before (refs 40, 41).

**Determination of Quantum Yield.** The photoisomerization quantum yield ( $\Phi$ ) of 12-F rhodopsin was determined relative to rhodopsin, of which the  $\Phi$  (0.65  $\pm$  0.02) and molar absorbance ( $\epsilon_{498} = 40,600 \pm 500 \text{ M}^{-1}\cdot\text{cm}^{-1}$ ) are well-established.<sup>56–59</sup> Rhodopsin and 12-F rhodopsin were solubilized in buffer A containing 10 mM DDM and 10 mM hydroxylamine to give an OD $\cdot\text{cm}^{-1}$  at 497 nm of 0.150  $\pm$  0.07. Samples were kept at 10 °C and showed no significant decrease of  $A_{497}$  after 2 h in the dark. Samples were illuminated through a 504  $\pm$  5 nm interference filter (Schott) such that the half time of bleaching was  $\geq$  30 min. Spectra were taken at intervals of 2–10 min. The data were converted to a straight line, the slope of which ( $S$ ) is a measure of the photosensitivity  $\epsilon_{504}\cdot\Phi$ , as described before.<sup>32,56</sup> Using the  $S$  of rhodopsin measured under identical conditions allows calculation of the  $\Phi$  of the analogue pigment.<sup>32</sup>

**Transducin Activation.** Activation of the rhodopsin-associated G protein transducin was determined at 20 °C using a fluorescence assay as described.<sup>60,61</sup> A hypotonic extract of isotonicity washed bovine rod outer segments served as the source of transducin.<sup>11</sup> Samples contained 2, 5, or 10 nM pigment and about 100 nM transducin in 20 mM HEPES, 100 mM NaCl, 2 mM MgCl<sub>2</sub>, 1 mM DTE, 0.01% (w/v) DDM, pH 7.4. Immediately before data acquisition a sample was illuminated for 5 min in bright white light, and when a steady fluorescence level was reached, GTP $\gamma$ S was added to a final concentration of 2.5  $\mu\text{M}$ . The initial rate in the increase in tryptophan fluorescence of the  $\alpha$ -subunit of transducin, induced by binding of GTP $\gamma$ S, was plotted against the pigment concentration, and the slope of the resulting straight line was rated against the slope obtained for rhodopsin in the same set of experiments.

## Results and Discussion

**Regeneration and Spectral Properties of the Corresponding Fluoro-rhodopsins.** In agreement with earlier data for the 12-F pigment,<sup>42</sup> fluoro substituents at position C<sub>10</sub>, C<sub>12</sub>, or C<sub>14</sub> only slightly reduced the rate of pigment formation, relative to that of unsubstituted 11-*cis* retinal, when incubated at a 2- to 3-fold molar excess with opsin. Exact rates were not measured, but pigment formation was 90–95% complete after a 2 h incubation at room temperature. When fluoropigment formation had leveled, no additional rhodopsin was generated upon subsequent incubation with 11-*cis* retinal, indicating that maximal pigment formation was achieved. From the resulting increase in absorbance at the peak wavelength relative to that obtained with 11-*cis* retinal in parallel experiments, the molar

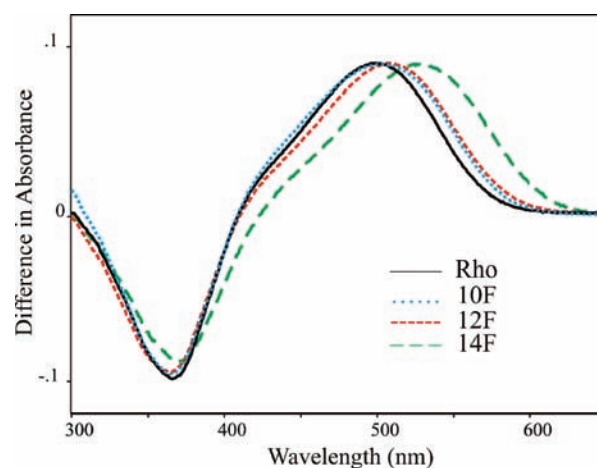


**Figure 2.** Spectral properties of native and fluoro rhodopsins prepared as described in the Experimental Section. Difference spectra were obtained by subtracting the spectrum after illumination from the dark-state spectrum. Illumination was performed in the presence of 10 mM hydroxylamine to ascertain full conversion of pigment, with production of the all-*trans* retinaloxime derivatives. The spectra were normalized at the maximal absorbance of the main absorbance band of the pigments near 500 nm.

absorbance ( $\epsilon_{\max}$ ) of the fluoropigments could be estimated with about 10% accuracy. The  $\epsilon_{\max}$  of 10-F and 14-F rhodopsin was similar to that of the native pigment (Table 1). However, the result for the 12-F analogue is an approximately 16% reduction in  $\epsilon_{\max}$  relative to rhodopsin, which in fact is in good agreement with the 18% reduction reported before.<sup>42</sup> A reduced oscillator strength can be deduced from Figure 2 for the free 12-F retinaloxime as well and hence probably is caused by a specific interaction between the 12-F substituent and the polyene system.

Earlier we reported a 6-fold reduction in regeneration rate for the 10-methyl pigment<sup>32</sup> and an at least 200-fold reduction with low incorporation level for the 12-methyl pigment.<sup>33</sup> It is most likely that their steric properties underlie this difference between the fluoro and methyl pigments. In 11-*cis* 10-methyl retinal it probably is due to an intrinsic ligand constraint, the steric interaction between the C<sub>10</sub>-methyl and the C<sub>13</sub>-methyl in the 12-*s trans* conformation dictated by the opsin binding pocket. Indeed, it was shown that the torsion in the C<sub>10</sub>–C<sub>13</sub> segment of retinal has significantly increased in 10-methyl rhodopsin.<sup>62</sup> In the case of 12-methyl retinal it probably reflects steric interaction of the methyl group with the backbone C=O oxygen of opsin residue Cys-187. According to the highest resolution structure available (2.2 Å<sup>63</sup>), the carbonyl oxygen C<sub>187</sub>–C=O is located at a distance of about 3.2 Å of C<sub>12</sub> pointing toward the C<sub>12</sub>-H bond under an angle of ca. 100°,

(56) Dartnall, H. J. A. In *Photochemistry of Vision, Handb. Sens. Physiol.*; Dartnall, H. J. A., Ed.; Springer-Verlag: Berlin, 1972; Vol. VII/1, pp 122–145.

(57) Hurley, J. B.; Ebrey, T. G.; Honig, B.; Ottolenghi, M. *Nature* **1977**, *270* (5637), 540–542.

(58) Birge, R. R.; Einterz, C. M.; Knapp, H. M.; Murray, L. P. *Biophys. J.* **1988**, *53* (3), 367–385.

(59) Kim, J. E.; Tauber, M. J.; Mathies, R. A. *Biochemistry* **2001**, *40* (46), 13774–13778.

(60) Phillips, W. J.; Cerione, R. A. *J. Biol. Chem.* **1988**, *263* (30), 15498–15505.

(61) Fahmy, K.; Sakmar, T. P. *Biochemistry* **1993**, *32*, 7229–7236.

(62) Verdegem, P. J. E.; Bovee-Geurts, P. H. M.; DeGrip, W. J.; Lugtenburg, J.; de Groot, H. J. M. *Biochemistry* **1999**, *38* (35), 11316–11324.

(63) Okada, T.; Sugihara, M.; Bondar, A.-N.; Elstner, M.; Entel, P.; Buss, V. *J. Mol. Biol.* **2004**, *342* (2), 571–583.

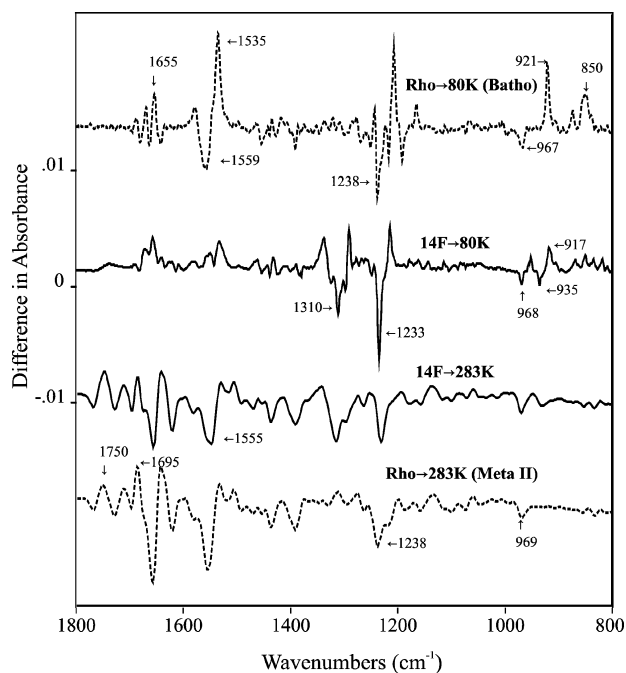


**Figure 3.** FT-IR difference spectra of native (dotted lines) and 14-F rhodopsin (continuous lines) and photoproducts generated by illumination at the temperatures indicated. Difference spectra were constructed by subtracting the dark-state spectrum from the spectrum obtained during 2 min after illumination. Negative bands represent vibrational bands characteristic for the dark state; positive bands represent characteristic vibrations of the photoproduct. The native Rho  $\rightarrow$  Batho difference spectrum taken at 80 K exhibits the typical, isolated HOOP pattern of Batho between 800 and 950  $\text{cm}^{-1}$ , reflecting the highly strained structure of the all-*trans* chromophore in Batho.

which allows about sufficient space for a fluoro substituent but is clearly within van der Waals distance of a methyl group (van der Waals radius of about 1.4 and 2.0 Å, respectively, bond length for C–F and C–CH<sub>3</sub> of 1.34 and 1.50 Å, respectively).

The peak absorbance in the visible region ( $\lambda_{\text{max}}$ ) we measure for the fluoro-pigments (Table 1) also is consistent with earlier data.<sup>38,41,42</sup> All fluoro-analogues exhibit a red shift of the main absorbance band relative to that of rhodopsin (Figure 2) that increases in the order 10-F < 12-F < 14-F, i.e., the closer the fluoro-substituent is located to the Schiff base, the larger the red shift. This is most likely due to destabilization of the ground state because of the perturbation of the charge distribution in the polyene positron by the fluoro substituent, which will have its largest effect at close range.

**Photochemistry and Activity of 14-F Rhodopsin.** Our FT-IR analyses agree with earlier data in that 14-F substitution does not significantly affect photoisomerization and signaling activity of rhodopsin.<sup>38–40</sup> The normal sequel of intermediates is observed, culminating in a final intermediate that shows the typical vibrational band pattern of Meta II in the 1550–1800  $\text{cm}^{-1}$  region (Figure 3, lower 14-F spectrum). A major effect of the 14-F substituent is the large upshift of the  $\text{pK}_a$  of the Meta I  $\leftrightarrow$  Meta II equilibrium (Figure 4, triangles), which was also observed for 14-F isorhodopsin.<sup>40</sup> This can be explained by the reduction in electronegativity of the Schiff base because of the electron withdrawing effect of the nearby fluoro substituent.<sup>44</sup>

In addition, it is expected that a 14-F substituent will also change the vibrational band pattern of the chromophore. This is indeed obvious in the 14-F Rho  $\rightarrow$  Batho and 14-F Rho  $\rightarrow$

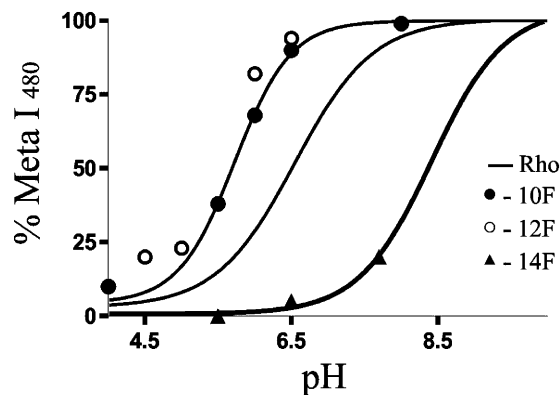


**Figure 4.** pH dependence of the Meta I  $\leftrightarrow$  Meta II equilibrium in native rhodopsin (solid line without data points) and the three fluoro analogues (symbolized as indicated) measured at 10 °C (283 K). The Rho and 14-F data could be fitted with a regular Henderson–Hasselbalch function. The 10-F and the 12-F data show a much steeper transition, which renders determination of a single  $\text{pK}_a$  value not reliable.

Meta II difference spectra (Figure 3), where the fingerprint region (C–C stretch vibrations) is split up into two sets of vibrations around 1233 and 1310  $\text{cm}^{-1}$ . A similar effect is observed for the chromophore HOOP vibrations in rhodopsin that are split in two bands at 968 and 935  $\text{cm}^{-1}$ . We postulate that the C<sub>7</sub>=C<sub>8</sub> A<sub>u</sub> HOOP vibration remains at 968  $\text{cm}^{-1}$ <sup>64–66</sup> and that the C<sub>11</sub>=C<sub>12</sub> A<sub>2</sub> HOOP vibration is downshifted to 935  $\text{cm}^{-1}$ . The pattern of isolated HOOP vibrations in Batho between 800 and 950  $\text{cm}^{-1}$  has also changed in 14-F Batho since the C<sub>14</sub>-H HOOP is lacking, which has a frequency of about 850  $\text{cm}^{-1}$  in native Batho (Figure 3, upper dotted spectrum). In contrast, the set of small bands around 1655  $\text{cm}^{-1}$ , representing the minor alterations in protein conformation accompanying the Rho  $\rightarrow$  Batho transition, shows a slightly different intensity distribution in the 14-F pigment, but no change in frequency distribution. Finally, it is noteworthy that the C–F stretch of ethylenic fluoro compounds appears as a medium strong vibration in the frequency range between 1050 and 1200  $\text{cm}^{-1}$  and is also quite sensitive to H-bonding and the polarity of its microenvironment.<sup>67–70</sup> However, in this frequency region we find no clear evidence for additional peaks in difference spectra between 14-F rhodopsin and its photointermediates, indicating that there is no obvious shift in intensity or frequency of the C<sub>14</sub>-F vibration during the photocascade.

**Photochemistry and Activity of 10-F Rhodopsin.** In contrast to 14-F substitution, the 10-F substituent exerts strong effects on the signaling activity of rhodopsin (Table 1, Figures 5 and 6). The photoisomerization process is not much affected, since the quantum yield is close to that of native rhodopsin<sup>38</sup> and the

(64) Eyring, G.; Curry, B.; Broek, A.; Lugtenburg, J.; Mathies, R. A. *Biochemistry* **1982**, *21* (2), 384–393.

(65) Palings, I.; VanDenBerg, E. M. M.; Lugtenburg, J.; Mathies, R. A. *Biochemistry* **1989**, *28*, 1498–1507.

(66) Lin, S. W.; Groesbeek, M.; Van der Hoef, I.; Verdegem, P. J. E.; Lugtenburg, J.; Mathies, R. A. *J. Phys. Chem. B* **1998**, *102* (15), 2787–2806.

(67) *The Sadtler Handbook of Infrared Spectra*; Sadtler Research Laboratories: Philadelphia, 1978.

(68) Eremenko, L. T.; Zhitomirskaya, N. G. *Izv. Akad. Nauk SSSR, Ser. Khim.* **1969**, *12*, 2631–2633.

(69) Buchhold, K.; Reimann, B.; Djafari, S.; Barth, H.-D.; Brutschy, B.; Tarakeshwar, P.; Kim, K. S. *J. Chem. Phys.* **2000**, *112* (4), 1844–1858.

(70) Kryachko, E. S.; Karpfen, A. *Chem. Phys.* **2006**, *329* (1–3), 313–328.

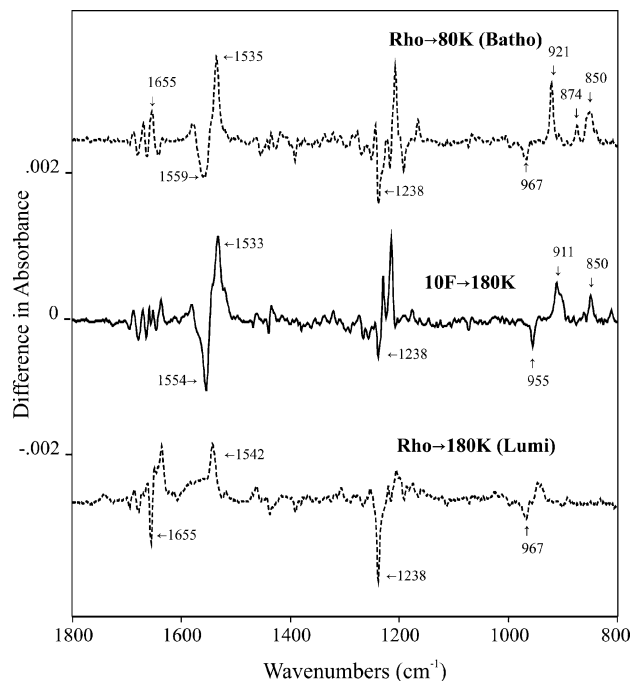


**Figure 5.** FT-IR difference spectra of native (dotted lines) and 10-F rhodopsin (continuous lines) and photoproducts generated by illumination at the temperatures indicated. Difference spectra were constructed by subtracting the dark-state spectrum from the spectrum obtained during 2 min after illumination. Negative bands represent vibrational bands characteristic for the dark state; positive bands represent characteristic vibrations of the photoproduct. The native Rho  $\rightarrow$  Batho difference spectra taken at 80 K shows the typical isolated HOOP pattern of Batho between 800 and 950  $\text{cm}^{-1}$ , reflecting the highly strained structure of the all-*trans* chromophore in Batho. This pattern represents the HOOPs from  $\text{C}_{11}\text{-H}$  (921  $\text{cm}^{-1}$ ),  $\text{C}_{10}\text{-H}$  (874  $\text{cm}^{-1}$ ),  $\text{C}_{12}\text{-H}$  (854  $\text{cm}^{-1}$ ),  $\text{C}_{14}\text{-H}$  (848  $\text{cm}^{-1}$ ), and  $\text{HC}_7=\text{C}_8\text{H}$  (838  $\text{cm}^{-1}$ ).

FT-IR difference spectrum of the 10-F Rho  $\rightarrow$  Batho transition (Figure 5, middle spectrum) is very similar to that of native rhodopsin, except for downshifts of HOOP vibrations and lack of the  $\text{C}_{10}\text{-H}$  HOOP, which is represented by the 874  $\text{cm}^{-1}$  vibration in the native spectrum (Figure 5, top spectrum). Again, we do not find evidence for additional peaks that may arise in a change of the  $\text{C}_{10}\text{-F}$  vibration between 10-F rhodopsin and photoproducts.

The effects of the 10-F substituent are most conspicuous in the temperature dependence of the thermal transitions (Batho  $\rightarrow$  Lumi  $\rightarrow$  Meta I  $\leftrightarrow$  Meta II) and in the  $\text{p}K_a$  of the Meta I  $\leftrightarrow$  Meta II equilibrium (Figures 4, 5, and 6). An upshift in all transition temperatures is observed. Typical Batho signals, normally decaying into Lumi at temperatures over 135 K, are still completely intact at 180 K in the case of the 10-F analogue (Figure 5). This increase in stability of the 10-F Batho intermediate corroborates earlier observations by electronic cryospectroscopy,<sup>43</sup> except that in that case 10-F Batho already started to decay near 150 K. Probably, this discrepancy originates in the different conditions applied. While our vibrational data were obtained for native membrane preparations, the visible spectroscopy was done on digitonin extracts in the presence of 66% glycerol, and a detergent environment usually reduces the activation barrier for conformational changes in membrane proteins.<sup>71,72</sup>

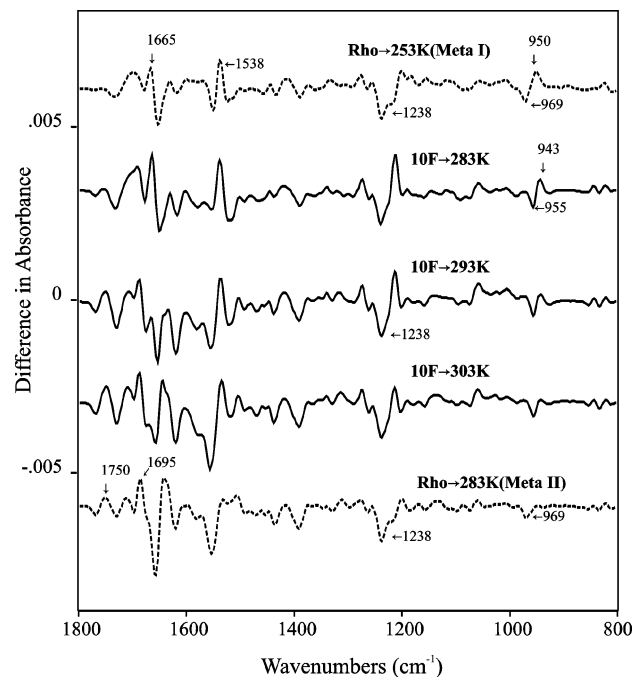


**Figure 6.** FT-IR difference spectra of native (dotted lines) and 10-F rhodopsin (continuous lines) and photoproducts generated by illumination at the temperatures indicated. Difference spectra were constructed by subtracting the dark-state spectrum from the spectrum obtained during 2 min after illumination. Negative bands represent vibrational bands characteristic for the dark state; positive bands represent characteristic vibrations of the photoproduct. The native spectra were taken at pH 5.5 to accentuate the differences between Meta I and Meta II. The 10-F spectra were taken at pH 6.5. The Meta I to Meta II difference spectra are stable over at least 12 min and hence represent the equilibrium state.

Similar observations were made for the Meta I to Meta II transition. Normally, Meta I decays into Meta II at temperatures over 255 K, under formation of a Meta I  $\leftrightarrow$  Meta II equilibrium with a temperature- and pH-dependent equilibrium constant.<sup>7,73,74</sup> However, 10-F Meta I is still stable at 10 °C and a pH of 6.5 (283 K; Figure 6) as evident from the typical Meta I vibrations at 1665, 1538, and 943  $\text{cm}^{-1}$ . Formation of 10-F Meta II is only clearly observed at temperatures  $\geq 20$  °C (293 K; Figure 6). Probably, the activation energy for the Meta I to Meta II transition has increased significantly, reducing the proportion of Meta II in the relevant temperature range relative to that in the native system. This aberrant behavior is further reflected in the  $\text{p}K_a$  of the Meta I  $\leftrightarrow$  Meta II equilibrium, which is significantly downshifted relative to native rhodopsin (Figure 4, filled circles). The decrease in  $\text{p}K_a$  observed for the 10-F analogue, in combination with the stronger temperature dependence of the Meta I  $\leftrightarrow$  Meta II equilibrium will be responsible for the strong reduction in signaling activity per photolyzed rhodopsin, to about 20% of that of native rhodopsin (Table 1). The signaling activity is assayed at 20 °C and pH 7.4, and under these conditions the 10-F analogue will strongly prefer the Meta I state.

The change in properties induced by 10-F substitution (thermal upshift of reaction cascade transitions and delayed formation of Meta II, leading to a significant lower G protein activation rate) is remarkably similar to those reported for 10-

(71) DeGrip, W. J. *Methods Enzymol.* **1982**, *81*, 256–265.

(72) Kusnetzow, A. K.; Altenbach, C.; Hubbell, W. L. *Biochemistry* **2006**, *45* (17), 5538–5550.

(73) Matthews, R. G.; Hubbard, R.; Brown, P. K.; Wald, G. J. *Gen. Physiol.* **1963**, *47*, 215–240.

(74) Parkes, J. H.; Gibson, S. K.; Liebman, P. A. *Biochemistry* **1999**, *38* (21), 6862–6878.



methyl rhodopsin.<sup>32</sup> Here as well, Batho is stable up to about 200 K, at pH 6.5 Meta II formation is only observed at temperatures  $\geq 20$  °C, and the G protein activation rate at 20 °C is strongly reduced, again to about 20% of native rhodopsin. Since a fluoro substituent is not much larger than hydrogen, but much smaller than a methyl group, it seems unlikely that steric effects are an important factor in the mechanism underlying the higher thermal stability of both the 10-F and 10-methyl photoproducts. Examination of the available Batho structure (PDB 2G87<sup>17</sup>) also does not reveal obvious candidates among the protein residues that would obstruct further relaxation of the twisted chromophore due to steric crowding with the additional methyl group at C<sub>10</sub>. The latter may have to cope with quite a weak interaction with the ring of Try-265, but that certainly would not be an issue for a fluoro substituent at C<sub>10</sub>. On the other hand, the fluoro and methyl substituent have in common a much higher molecular mass relative to hydrogen, and a mass effect therefore could be a common denominator in their effect on the photocascade. That may imply that relaxation of the twisted all-*trans* chromophore in the Batho to BSI transition would involve further localized rotation of the C<sub>10</sub>-H element. It has been argued that the additional mass of the methyl group in 12-methyl rhodopsin would slow down the rotational movement of the C<sub>12</sub>-H element and thereby the rate of photoisomerization, which can explain the decrease in quantum yield.<sup>33</sup> In a similar way, the additional mass in 10-F and 10-methyl Batho may increase the activation barrier for further relaxation of the chromophore. This would corroborate time-resolved resonance Raman observations, indicating that decay of Batho involves further relaxation of the C<sub>10</sub>-C<sub>12</sub> unit of the chromophore.<sup>16,75</sup> It would be interesting to see whether computational and molecular dynamics studies will be able to shed more light on this issue.

Remains the observation that the 10-F and 10-methyl substituents also have profound effects on the temperature dependence of the Meta I  $\leftrightarrow$  Meta II equilibrium. This transition involves a variety of protein conformational changes,<sup>2,10,48,49,74,76-85</sup> and it is hard to imagine that the additional mass of a fluoro or methyl substituent in the ligand could play a major role here, unless additional rotational rearrangement in the ligand is involved,

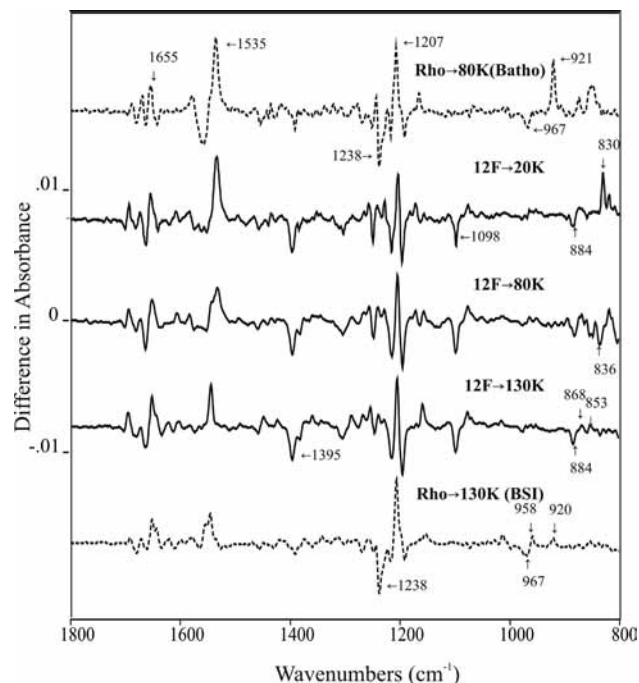


**Figure 7.** FT-IR difference spectra of native (dotted lines) and 12-F rhodopsin (continuous lines) and photoproducts generated by illumination at the temperatures indicated. Difference spectra were constructed by subtracting the dark-state spectrum from the spectrum obtained during 2 min after illumination. Negative bands represent vibrational bands characteristic for the dark state; positive bands represent characteristic vibrations of the photoproduct. Native Rho  $\rightarrow$  Batho difference spectra taken at 20 or 80 K are identical and exhibit the typical, isolated HOOP pattern of Batho between 800 and 950  $\text{cm}^{-1}$ , reflecting the highly strained structure of the all-*trans* chromophore in Batho. The 12-F spectra present unique, strong vibrations at 1395 and 1098  $\text{cm}^{-1}$ , which derive from the 12-F rhodopsin state, and are further discussed in the text.

for which there is some evidence.<sup>86</sup> Alternatively, these substituents could be at a critical position in the ligand to impair by steric interaction (methyl substituent) or by dipolar interaction (fluoro substituent) the H-bonding network rearrangements accompanying Meta II formation.

**Photochemistry and Activity of 12-F Rhodopsin.** The most diverse intriguing effects are observed upon 12-F substitution (Figures 7 and 8) and involve perturbation of photoisomerization as well as of signaling activity of rhodopsin. The quantum yield shows the largest decrease among the three fluororhodopsins studied here (Table 1). This is a strong indication that the rate of the photoisomerization process is significantly reduced only in the 12-F analogue. In addition, the G protein activation rate is strongly reduced as well, to about 32% of that of rhodopsin (Table 1).

The quantum yield we measure for the 12-F pigment (0.47) is substantially lower than that of the 12-methyl pigment (0.55).<sup>33</sup> An important factor is probably the larger mass of the fluoro substituent in comparison to a methyl group (19 and 15 Da, respectively), which according to the same argument mentioned above and detailed before<sup>33</sup> would further slow down the out-of-plane rotational movement of this C<sub>12</sub> bond, essential for driving the photoisomerization process, and hence would further reduce the quantum yield. It is questionable however, whether this could lead to the substantial decrease in quantum

- (75) Pan, D. H.; Ganim, Z.; Kim, J. E.; Verhoeven, M. A.; Lugtenburg, J.; Mathies, R. A. *J. Am. Chem. Soc.* **2002**, *124* (17), 4857–4864.  
 (76) Lamola, A. A.; Yamane, T.; Zipp, A. *Biochemistry* **1974**, *13* (4), 738–745.  
 (77) DeGrip, W. J.; Gray, D.; Gillespie, J.; Bovee-Geurts, P. H. M.; VanDenBerg, E. M. M.; Lugtenburg, J.; Rothschild, K. J. *Photochem. Photobiol.* **1988**, *48*, 497–504.  
 (78) Farrens, D. L.; Altenbach, C. A.; Yang, K.; Hubbell, W. L.; Khorana, H. G. *Science* **1996**, *274* (5288), 768–770.  
 (79) Sheikh, S. P.; Zvyaga, T. A.; Lichtarge, O.; Sakmar, T. P.; Bourne, H. R. *Nature* **1996**, *383* (6598), 347–350.  
 (80) Klein-Seetharaman, J.; Hwa, J.; Cai, K. W.; Altenbach, C. A.; Hubbell, W. L.; Khorana, H. G. *Biochemistry* **1999**, *38* (25), 7938–7944.  
 (81) Hubbell, W. L.; Altenbach, C.; Hubbell, C. M.; Khorana, H. G. *Adv. Prot. Chem.* **2003**, *63*, 243–290.  
 (82) Scheerer, P.; Park, J. H.; Hildebrand, P. W.; Kim, Y. J.; Krauss, N.; Choe, H.-W.; Hofmann, K. P.; Ernst, O. P. *Nature* **2008**, *455* (7212), 497–502.  
 (83) Ahuja, S.; Crocker, E.; Eilers, M.; Hornak, V.; Hirshfeld, A.; Ziliox, M.; Syrett, N.; Reeves, P. J.; Khorana, H. G.; Sheves, M.; Smith, S. O. *J. Biol. Chem.* **2009**, *284* (15), 10190–10201.  
 (84) Angel, T. E.; Chance, M. R.; Palczewski, K. *Proc. Natl. Acad. Sci. U.S.A.* **2009**, *106* (21), 8555–8560.  
 (85) Angel, T. E.; Gupta, S.; Jastrzebska, B.; Palczewski, K. *Proc. Natl. Acad. Sci. U.S.A.* **2009**, *106* (34), 14367–14372.

- (86) DeLange, F.; Bovee-Geurts, P. H. M.; Pistorius, A. M. A.; Rothschild, K. J.; DeGrip, W. J. *Biochemistry* **1999**, *38* (40), 13200–13209.

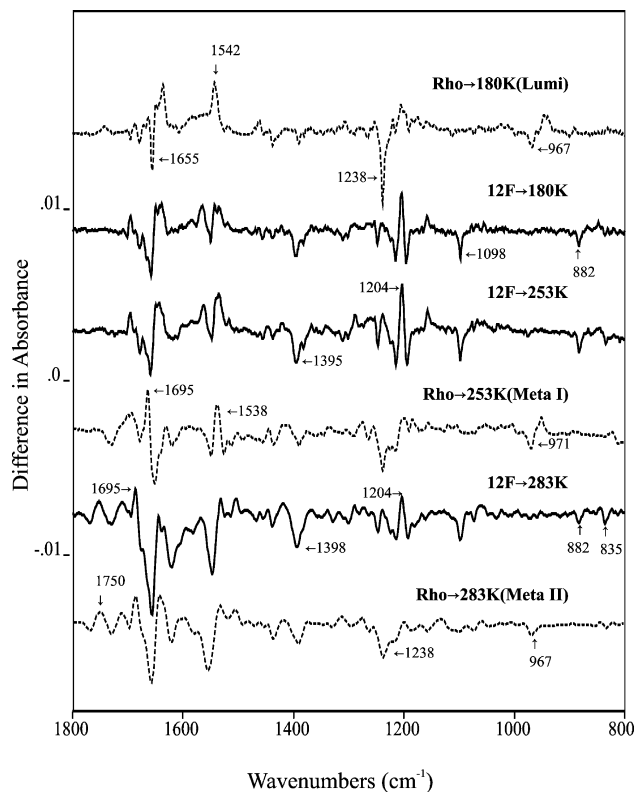


**Figure 8.** FT-IR difference spectra of native (dotted lines) and 12-F rhodopsin (continuous lines) and photoproducts generated by illumination at the temperatures indicated. Difference spectra were constructed by subtracting the dark-state spectrum from the spectrum obtained during 2 min after illumination. Negative bands represent vibrational bands characteristic for the dark state; positive bands represent characteristic vibrations of the photoproduct. The 12-F spectra present unique, strong vibrations at 1395 and 1098  $\text{cm}^{-1}$ , which derive from the 12-F rhodopsin state, and are further discussed in the text.

yield we have measured (0.55  $\rightarrow$  0.47). An additional factor may be dipolar and/or H-bonding interaction of the fluoro substituent with its microenvironment, for which we have indirect evidence (see below), that might dampen or counteract this out-of-plane rotation and thereby also impair the rate of isomerization.

We observe mixed effects of 12-F substitution on the photocascade. At 80 K no typical Batho pattern was observed, in as far as the characteristic and stable HOOP vibrations in the 800–930  $\text{cm}^{-1}$  region are absent (Figure 7, middle 12-F spectrum). Instead, this region was quite noisy and not very reproducible between experiments. However, we did observe stable HOOP vibrations when we cooled down to 20 K before illumination. In fact, the 20 K photoproduct of 12-F rhodopsin has all the characteristics of Batho. Typical for 12-F Batho are the downshifted HOOP vibrations and the absence of the 12-HOOP, in native Batho present as an 850  $\text{cm}^{-1}$  vibration (Figure 5, top spectrum). For instance, the strong Batho 11-HOOP has shifted from 921 to 830  $\text{cm}^{-1}$  (Figure 7, top 12-F spectrum). Likewise, the  $\text{C}_7=\text{C}_8$  and  $\text{C}_{11}$  HOOPs in 12-F rhodopsin have shifted to 884 and 836  $\text{cm}^{-1}$ . This is most obvious in the 12-F difference spectra at 80 and 283 K (Figure 7, top 12-F and Figure 8, bottom 12-F spectrum, respectively), since in the other spectra the 836  $\text{cm}^{-1}$  peak is less evident because of partial overlap with positive peaks in the photoproduct.

The unstable pattern between 800 and 900  $\text{cm}^{-1}$  in the 12-F photoproduct at 80 K has not been described before, to our

knowledge. We reasoned that it might represent a transition state between Batho and the next intermediate. Therefore we performed similar analyses for native and 12-F rhodopsin at 130 and 135 K, a temperature trajectory where Batho was reported to directly decay into Lumi.<sup>12,13</sup> The BSI intermediate has been observed by cryotrapping only in rhodopsin analogues so far, since in rhodopsin the Batho to BSI transition is entropy-driven and at low temperatures the equilibrium strongly prefers the Batho state.<sup>87–91</sup> Unexpectedly, we encountered a condition where illumination of native rhodopsin (2 min, OG530 cutoff filter, 130 K) produced a photoproduct with a, compared to Batho, slightly changed protein pattern around 1650  $\text{cm}^{-1}$ , a quite different  $\text{C}=\text{C}$  stretch pattern around 1550  $\text{cm}^{-1}$  and a shifted and strongly reduced HOOP pattern between 800 and 950  $\text{cm}^{-1}$  (Figure 7, bottom spectrum). This typical pattern had fully developed at about 4 min after illumination and remained stable for at least 6 min, and is quite reminiscent of that observed for the BSI intermediate in analogues of rhodopsin by FT-IR cryospectroscopy and in native rhodopsin by time-resolved resonance Raman spectroscopy at 7  $^{\circ}\text{C}$ .<sup>75,88,92</sup> Hence, we assume this is the first demonstration of native BSI by cryotrapping. Interestingly, applying the same conditions to the 12-F pigment resulted in a photoproduct with very similar characteristics to native BSI, taking the strong, 12-F inflicted downshift of the HOOP vibrations into account. Therefore, we assign this to the 12-F BSI intermediate, implying that illumination of 12-F rhodopsin generates a 12-F Batho analogue that is stable at 20 K but not at 80 K and at 130 K rapidly decays into the 12-F BSI analogue. When comparing the 12-F difference spectra at 20, 80, and 130 K (Figure 7), only minor changes in protein pattern around 1650  $\text{cm}^{-1}$  and in fingerprint pattern around 1200  $\text{cm}^{-1}$  are obvious, while there is a clear frequency shift in the  $\text{C}=\text{C}$  pattern near 1540  $\text{cm}^{-1}$  and a frequency shift and intensity change in the HOOP pattern between 800 and 870  $\text{cm}^{-1}$ . The overall pattern at 80 K seems to be a mixture of that at 20 and at 130 K, as is evident in particular in the  $\text{C}=\text{C}$  and fingerprint patterns. Our interpretation is that 12-F Batho is in equilibrium with 12-F BSI with a temperature-dependent equilibrium constant, which is still very small at 20 K and has become very large at 130 K. Similar to the native system the transition from 12-F Batho to 12-F BSI mainly involves vibrational alterations in the chromophore, reflecting further relaxation of the highly strained conformation.<sup>14,75</sup> The temperature dependence of this equilibrium is strongly affected by the 12-F substitution, however, which suggests that the enthalpic component of this equilibrium has increased its weight. It points at a higher thermal stability of 12-F BSI relative to that of 12-F Batho as compared to the native situation, which may also bear on the higher stability of the 12-F Lumi intermediate relative to native Lumi, described below.

Our data can explain results from an early study on the photocascade of 12-F rhodopsin, employing UV–vis cryospec-

- (87) Hug, S. J.; Lewis, J. W.; Einterz, C. M.; Thorgeirsson, T. E.; Kliger, D. S. *Biochemistry* **1990**, *29* (6), 1475–1485.
- (88) Ganter, U. M.; Kashima, T.; Sheves, M.; Siebert, F. *J. Am. Chem. Soc.* **1991**, *113*, 4087–4092.
- (89) Randall, C. E.; Lewis, J. W.; Hug, S. J.; Bjorling, S. C.; Eisnerhanas, I.; Friedman, N.; Ottolenghi, M.; Sheves, M.; Kliger, D. S. *J. Am. Chem. Soc.* **1991**, *113*, 3473–3485.
- (90) Mah, T. L.; Lewis, J. W.; Sheves, M.; Ottolenghi, M.; Kliger, D. S. *Photochem. Photobiol.* **1995**, *62* (2), 356–360.
- (91) Strassburger, J. M.; Gärtner, W.; Braslavsky, S. E. *Biophys. J.* **1997**, *72* (5), 2294–2303.
- (92) Wang, Y.-J.; Bovee-Geurts, P. H. M.; Lugtenburg, J.; DeGrip, W. J. *Photochem. Photobiol.* **2008**, *84* (4), 889–894.



troscopy, which concluded that progress and temperature dependence of the photointermediates were very similar to that of rhodopsin, converse to our results.<sup>43</sup> In this case this discrepancy is probably not mainly due to the less natural experimental conditions employed in that study (digitonin solubilized pigment, cryoprotected with 66% glycerol). In fact, close inspection of the published data reveals that at 82 K, the lowest temperature investigated, the  $\lambda_{\text{max}}$  of the photosteady-state mixture is red-shifted by only 3 nm relative to that of 12-F rhodopsin, much less than in the case of native rhodopsin (ca. 14 nm), and the extent of 12-F Batho formation seems to be much smaller than with native rhodopsin. In line with our data, we can now interpret this in the sense that at 82 K a mixture of 12-F rhodopsin, 12-F Batho, and 12-F BSI is present, which reduces the red shift of the  $\lambda_{\text{max}}$  of the photomixture as well as the proportion of Batho, relative to the situation for native rhodopsin where BSI is not generated. At temperatures over 130 K, 12-F BSI will then decay into 12-F Lumi. In this way, the results of both studies can be reconciled.

At 180 K the 12-F photoproduct exhibits a typical Lumi pattern, similar to native (Figure 8, two top spectra). This is for instance apparent in the change in C=C and fingerprint patterns and in the simple HOOP pattern, as compared to Batho, reflecting a more relaxed all-*trans* chromophore, and in the strong 1655 cm<sup>-1</sup> signal reflecting changes in the interaction between the protonated Schiff base and the counterion (Glu-113).<sup>93–95</sup> Remarkably, in the 12-F system this pattern persists at 253 K, where normally Meta I has been formed (Figure 8, two middle spectra). This indicates that 12-F Lumi is thermally more stable than native Lumi. Since a similar situation seems to pertain to 12-F BSI, one explanation could be that the 12-F substituent in the more relaxed all-*trans* chromophore is interacting weakly with protein elements lining the binding site. This will be discussed in more detail below. At temperatures over 273 K a typical pH-dependent Meta I ↔ Meta II equilibrium is observed for the 12-F system by UV–vis spectroscopy (Figure 4), and at 283 K (10 °C) and pH 5.5 the typical Meta II pattern is clearly present in FT-IR difference spectra (Figure 8, two bottom spectra). We conclude that the temperature dependence of the Meta I ↔ Meta II equilibrium is not markedly perturbed by 12-F substitution.

Another major difference with the native system lies in the large shift in the pH dependence of the 12-F Meta I ↔ Meta II equilibrium (Figure 4, open circles). Such shifts are observed for many retinal derivatives,<sup>32,33,40,50,92,95–98</sup> and it explains the lower signaling activity of 12-F rhodopsin relative to native rhodopsin, since this activity is assayed at 20 °C and pH. 7.4, conditions where the relative proportion of 12-F Meta II is much lower than that of native Meta II. At 10 °C the pH dependence curve of the 12-F Meta I ↔ Meta II equilibrium is even further shifted away from native than that of 10-F. Nevertheless, the signaling activity of 12-F rhodopsin surpasses that of 10-F rhodopsin (Table 1). The reason probably lies in the unfavorable

temperature dependence of the Meta I ↔ Meta II equilibrium in the 10-F pigment that will only slowly increase the proportion of Meta II at increasing temperature.

Among the three fluoroderivatives studied in this paper, the 12-F pigment shows two unique features in the FT-IR difference spectra with its photoproducts. Those are the strong rhodopsin peaks at 1395 and 1098 cm<sup>-1</sup> (Figures 7 and 8). We have not been able to assign the 1395 cm<sup>-1</sup> vibration yet and cannot exclude that it reflects an increase in intensity of the small peak at about the same frequency already present in the native FT-IR difference spectra, which probably represents the 13-methyl symmetric deformation.<sup>66</sup> The strong vibration at 1098 cm<sup>-1</sup> is a novel feature, however, and most likely represents the C–F stretch vibration in the rhodopsin state. In free 12-F 11-*cis* retinal we have observed an among retinals unique medium strong vibration at 1084 cm<sup>-1</sup> (not shown) and tentatively assign this to the C<sub>12</sub>–F stretch. The shift in frequency and strong intensity in rhodopsin can be due to several factors. For instance, in rhodopsin the chromophore is twisted around the C<sub>11</sub>=C<sub>12</sub> and the *s-trans* C<sub>12</sub>–C<sub>13</sub> bonds. Further, we modeled a fluoro-atom at position C<sub>12</sub> in the rhodopsin structure (1U19<sup>63</sup>) and this seems to experience quite a polar environment with a distance of 2.5–3 Å to a nearby water molecule (wat2014) and about 2.5 Å to the carbonyl oxygen of Cys-187. Dipolar and/or H-bond interaction with these constituents in the protein structure may also explain the relative strong downshift reported for the 12-F resonance in early F-NMR studies (chemical shift of –92 ppm for 12-F rhodopsin versus –107 ppm for free 11-*cis* 12-F retinal<sup>42,99</sup>). During the photoisomerization process the C–F bond rotates and the fluoro substituent moves away from this polar environment. Taking the published Batho structure (2G87<sup>17</sup>) we estimate that the F atom has moved away over at least 1 Å from the water molecule and the C<sub>187</sub> C=O and has moved toward the C<sub>β</sub> of Ala-117. Rearrangements in at least three internal water molecules during the rhodopsin to Batho transition have been well documented.<sup>100</sup> A corresponding change in dipolar interactions may contribute to a frequency shift and/or change in intensity of the C–F vibration.

In addition, close juxtaposition of the 12-F atom to the C<sub>β</sub> of Ala-117 may destabilize the 12-F Batho state, facilitating the transition to 12-F BSI. However, in the absence of sufficiently high-resolution structures of Batho and later intermediates, the molecular mechanism underlying the various effects of 12-F substitution on the photocascade remains speculative.

In contrast to substitution at C<sub>10</sub>, quite different patterns are observed for methyl and fluoro substitution at C<sub>12</sub>. As discussed above, we attribute the difference in the photoisomerization process of the 12-methyl and 12-F pigments to the distinction in mass and polarity of the two substituents. The remarkable deviation in the subsequent reaction cascade of the 12-methyl pigment,<sup>33</sup> we rather attribute to steric effects. A methyl group at C<sub>12</sub> will encounter severe steric interaction in the Batho state with C<sub>β</sub> of Ala-117 and also with the backbone C=O of the same residue. This will probably force the photoactivated binding pocket to first relay photon energy into a different strain distribution in the chromophore and subsequently dissipate it through an altered conformational pathway in the protein moiety. The markedly distinct FT-IR difference spectra observed through the entire 12-methyl photocascade<sup>33</sup> would concur with such a

(93) Ganter, U. M.; Gärtner, W.; Siebert, F. *Biochemistry* **1988**, *27* (19), 7480–7488.

(94) Pan, D. H.; Mathies, R. A. *Biochemistry* **2001**, *40* (26), 7929–7936.

(95) Lüdeke, S.; Fonfria, V. A. L.; Siebert, F.; Vogel, R. *Biopolymers* **2006**, *83* (2), 159–169.

(96) Vogel, R.; Siebert, F.; Lüdeke, S.; Hirshfeld, A.; Sheves, M. *Biochemistry* **2005**, *44* (35), 11684–11699.

(97) Bartl, F. J.; Fritze, O.; Ritter, E.; Herrmann, R.; Kuksa, V.; Palczewski, K.; Hofmann, K. P.; Ernst, O. P. *J. Biol. Chem.* **2005**, *280* (40), 34259–34267.

(98) Vogel, R.; Lüdeke, S.; Siebert, F.; Sakmar, T. P.; Hirshfeld, A.; Sheves, M. *Biochemistry* **2006**, *45* (6), 1640–1652.

(99) Liu, R. S. H.; Colmenares, L. U. *Proc. Natl. Acad. Sci. U.S.A.* **2003**, *100* (25), 14639–14644.

(100) Kandori, H.; Maeda, A. *Biochemistry* **1995**, *34* (43), 14220–14229.

situation. For instance, at 80 K the vibrational patterns of both protein and chromophore are markedly altered as compared to those of the native as well as the 12-F rhodopsin, and there is no evidence for intensified HOOP vibrations in the photoproduct. Both the protein and chromophore patterns remain very atypical at later stages in the 12-methyl photocascade, a normal Meta II intermediate is not observed and signaling activity is practically absent.<sup>33</sup> A novel feature, a medium strong positive peak at  $1003\text{ cm}^{-1}$ , was observed at early stages in the 12-methyl cascade and was tentatively assigned to a  $C_{12}$ -methyl wag.<sup>33</sup> This would agree with our present perspective that steric interaction of the  $C_{12}$ -methyl group with protein residues dominates the fate of the photocascade of 12-methyl rhodopsin.

### Summary

Inspired by the strongly perturbing action of 10-methyl and 12-methyl substituents on photocascade and signaling activity of rhodopsin, we here report on the corresponding fluoro derivatives that also add significant mass to the chromophore, but are much smaller in size. The 14-F derivative did not significantly impair rhodopsin properties, in agreement with earlier studies,<sup>38,40,41</sup> indicating that fluoro substitution by itself need not have a perturbing action. However, both 10-F and 12-F substitution have complex effects on several rhodopsin properties.

A common effect is that they both significantly reduce the signaling activity to 20 and 32% of native rhodopsin, respectively. As such, the 10-F and 12-F all-*trans* chromophore both classify as partial agonists. A major cause of this lower activity is a significant downshift of the pH-sensitivity curve of the Meta I  $\leftrightarrow$  Meta II equilibrium (Figure 4), resulting in a substantial decrease in the proportion of the active Meta II state generated at physiological pH. Such a downshift is a common feature in modified chromophores, but the underlying molecular mechanism is still unclear and more detailed structural information on all photointermediates is needed.

Quite different are the effects of 10-F and 12-F substitution on the photochemical properties of rhodopsin. Since speed and efficiency of the photoisomerization process are closely correlated,<sup>16,45,46</sup> the quantum yield is a good measure for the overall performance of the process. In view of this it appears that photoisomerization is only substantially perturbed by 12-F substitution. We propose that this is largely due to a mass effect, requiring more energy to perform the out-of-plane rotational movement of the  $C_{12}$ -F bond that initiates a coherent path over the excited state energy surface toward a perturbed 11-*transoid* configuration. This is similar to our explanation for the decrease in quantum yield of the 12-methyl pigment.<sup>33</sup> An additional factor in the 12-F pigment, we propose, is dipolar interaction between the fluoro substituent and nearby elements in the protein

structure, which may further slow down the out-of-plane rotation and reduce the quantum yield.

The reaction cascade following photoisomerization into Batho is affected both by 10-F and by 12-F substitution. The effect of 12-F substitution is relatively minor, however. It is probably connected to specific interactions of the 12-F moiety with its environment that affect the thermal stability of Batho and Lumi, but eventually a Meta II state is generated in the normal temperature range. On the contrary, 10-F substitution has pronounced effects in the sense that the temperature range of all transitions is shifted upward substantially. Considering the small additional size of a fluoro substituent over hydrogen it is unlikely that steric crowding is a major issue here. Further, the same phenomenon is also observed with the 10-methyl pigment,<sup>32</sup> and the most obvious property these substituents have in common, is their much larger mass than hydrogen. This would suggest that specific conformational relaxation and rearrangement steps continue in the chromophore up to formation of Meta II, and that a local increase of mass may put an additional energy requirement in the early transitions of the reaction cascade.

Our data again illustrate the very subtle interplay between a ligand and its cognate G protein coupled receptor and extend the examples that small modifications in the ligand can modify this interplay and thereby redirect the conformational space and at the same time the activity profile of the receptor. In addition our results allow the conclusion that the  $C_{12}$ -H element of the rhodopsin chromophore is a major rate-limiting factor in the photoisomerization process leading to a strained 11-*trans* chromophore in Batho, in support of current theories on the molecular mechanism of this process.<sup>15,16,25,26,28,29,33,46</sup> On the other hand, the  $C_{10}$ -H element seems to play a dominant role in the relaxation and further rearrangement of the strained chromophore during the thermal reactions following decay of Batho.

**Acknowledgment.** We thank Dr. Rosalie Crouch (Medical University of South Carolina, Charleston) for a generous gift of 11-*cis* retinal. Dr. Gert Vriend (Centre for Molecular BioInformatics CMBI, Radboud University Nijmegen Medical Centre, The Netherlands) is acknowledged for expert assistance with interpretation of the rhodopsin and bathorhodopsin structures using What-If-YASARA ([www.yasara.org](http://www.yasara.org)). We thank Dr. Arthur Pistorius (Radboud University Nijmegen Medical Centre) for generating rhodopsin models containing the fluoro substituents. This research was supported by The Netherlands Foundation for Scientific Research through its Chemical Council (NWO-CW) and by the EC (E-MeP, contract LSHG-CT-2004-504601).

JA907577P